

Crystal Structure Determination of $\text{BaNd}_2\text{Ti}_3\text{O}_{10}$ Using High-Resolution Electron Microscopy

A. OLSEN

*Institute of Physics, University of Oslo, P.O. Box 1048,
0316 Oslo 3, Norway*

AND R. S. ROTH

National Bureau of Standards, Washington, D.C. 20234

Received February 25, 1985; in revised form May 31, 1985

The crystal structure of $\text{BaNd}_2\text{Ti}_3\text{O}_{10}$ has been determined by electron diffraction and high-resolution electron microscopy. The unit cell is monoclinic with $P2_1/m$ as the most probable space group and not orthorhombic as previously found by X-ray diffraction. However, the structure has an orthorhombic pseudosymmetry, but due to the small Nd^{3+} cations the octahedra are tilted and the structure is monoclinic. The cell dimensions based on X-ray data are: $a_m = 7.7310 \pm 0.0006 \text{ \AA}$; $b_m = 7.6661 \pm 0.0007 \text{ \AA}$; $c_m = 14.210 \pm 0.002 \text{ \AA}$; $\beta_m = 97.82 \pm 0.01^\circ$. © 1985 Academic Press, Inc.

Introduction

Ceramics in the $\text{BaO-Nd}_2\text{O}_3\text{-TiO}_2$ system are characterized by high-temperature stability, high permittivity, and low dielectric losses and have important electronic applications (1). During a study of these ceramics Kolar, Gaberscek, Volavsek, Parker, and Roth (2) discovered two new ternary compounds. By a combination of metallography, electron microanalysis, and X-ray diffraction one of the compounds was identified as $\text{BaNd}_2\text{Ti}_3\text{O}_{10}$. According to preliminary single crystal X-ray data this phase was found to be C-centered orthorhombic. The cell dimensions were determined using X-ray powder diffraction. A least-squares refinement gave the following values: $a_0 = 3.8655 \pm 0.0003 \text{ \AA}$; $b_0 = 28.156 \pm 0.003 \text{ \AA}$; $c_0 = 7.6661 \pm 0.0007 \text{ \AA}$. The rules for possible reflections were

found to be: $hkl: h + k = 2n; h0l: l = 2n$. Three space groups were possible: No. 36 $Cmc2_1$, No. 40 $C2cm$ and No. 63 $Cmcm$. Subsequent studies of this compound using electron diffraction showed, however, weak extra reflections which could not be explained according to the C-centered orthorhombic cell.

The present paper reports the structure determination of this compound using high-resolution electron microscopy and electron diffraction. Due to the two short orthorhombic axes this compound was particularly suitable for this technique and a model for the structure could be determined directly from the images.

Experimental

The preparation of the $\text{BaNd}_2\text{Ti}_3\text{O}_{10}$ compound has been described previously by

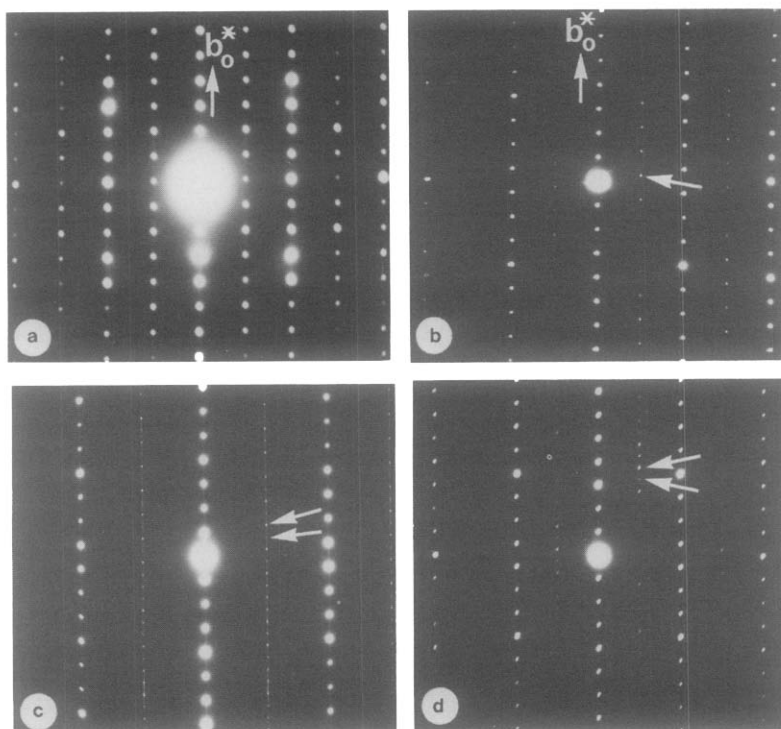


FIG. 1. Electron diffraction pattern of: (a) $[100]_o$, (b) $[001]_o$, (c) $[201]_o$, and (d) $[001]_o$ projections from $\text{BaNd}_2\text{Ti}_3\text{O}_{10}$.

Kolar *et al.* (2). Specimens suitable for electron microscopy were prepared by two methods. Some crystals were crushed into fine fragments and placed on holey carbon supporting films. The crystals have an extremely good cleavage normal to the long b_o axis. In order to study projections with the b_o axis normal to the incident electron beam, some crystals were polished mechanically as thin as possible and subsequently thinned by ion-etching. The specimens were studied at 100 kV in a JEOL electron microscope equipped with a top-entry high-resolution goniometer stage.

Electron Diffraction

Electron diffraction patterns showed weak extra reflections which could not be explained according to the C -centered

orthorhombic cell. These weak reflections are shown in three of the electron diffraction patterns in Fig. 1. All the reflections in the $[100]_o$ projection in Fig. 1a can be indexed according to the C -centered orthorhombic unit cell. However, in the $[001]_o$ and $[201]_o$ projections shown in the Figs. 1b–d there are weak reflections (indicated by arrows) which cannot be indexed according to the orthorhombic unit cell. These reflections indicate a monoclinic structure (see Fig. 2). The electron diffraction pattern in Figure 1b comes from an area with one orientation of the monoclinic cell. Figure 1d comes from an area with two orientations of the structure as indicated by the two sets of weak reflections. Diffuse streaks parallel to b_o^* were sometimes observed (Fig. 1c). These streaks go through all reflections including the central spot.

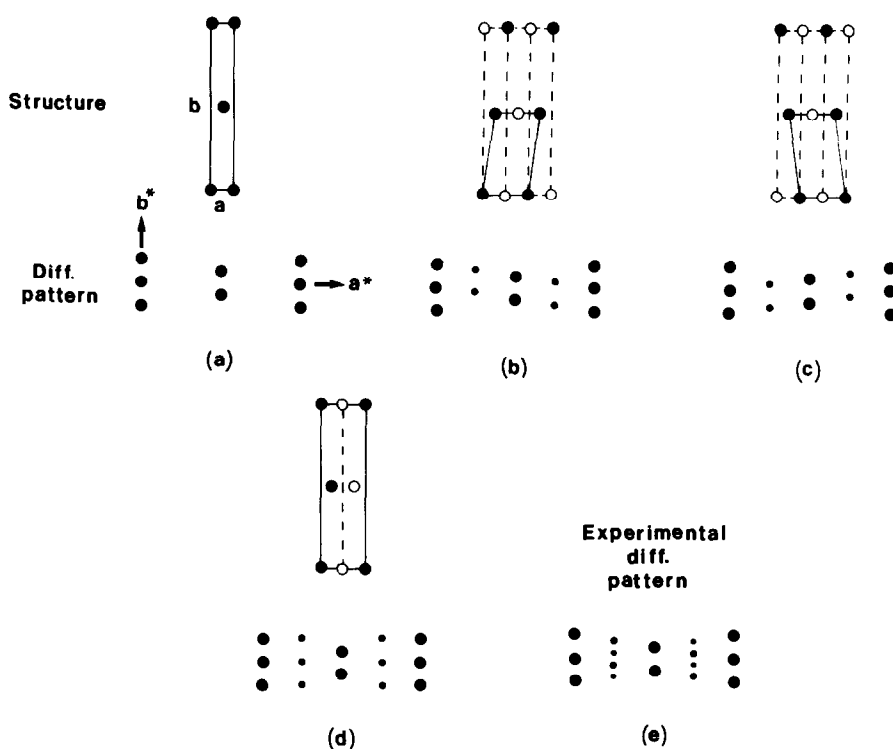


FIG. 2. Schematic diffraction patterns and the associated lattice types used for the derivation of the monoclinic unit cell of BaNd₂Ti₃O₁₀.

This indicates that the streaks are crystal form effects and due to thin crystal plates. The weak extra reflections were later found in single crystal X-ray patterns using very long exposures.

A schematic interpretation of the electron diffraction patterns is given in Fig. 2. It is shown how a C-centered orthorhombic lattice can transform to a monoclinic lattice. If the two lattice points in the C-centered orthorhombic lattice in Fig. 2a become slightly different as indicated in Fig. 2b, weak extra reflections appear. Figure 2c shows that a different unit cell orientation is possible. If the two orientations are distributed in a periodic way, a larger orthorhombic unit cell may also be possible as shown in Fig. 2d. However, the resulting diffraction pattern is not consistent with the present experimental observations. On the

other hand, a disordered mixture of the two orientations (Figs. 2b and c) can explain the experimental diffraction patterns in Fig. 1. This is demonstrated in Fig. 2e.

If \mathbf{a}_o , \mathbf{b}_o , \mathbf{c}_o are lattice vectors of the orthorhombic unit cell previously determined by X-ray diffraction (2) and \mathbf{a}_m , \mathbf{b}_m , \mathbf{c}_m the vectors of the monoclinic cell, the following relations hold:

$$\begin{aligned} \mathbf{a}_m^* &= \frac{1}{2}(\mathbf{a}_o^* + \mathbf{b}_o^*), & \mathbf{b}_m^* &= \mathbf{c}_o^*, & \mathbf{c}_m^* &= 2\mathbf{b}_o^* \\ \mathbf{a}_m &= 2\mathbf{a}_o, & \mathbf{b}_m &= \mathbf{c}_o, & \mathbf{c}_m &= \frac{1}{2}(-\mathbf{a}_o + \mathbf{b}_o). \end{aligned} \quad (1)$$

Crystal Structure

Because the extra reflections violating the orthorhombic symmetry are very weak, the structure could be determined to a first approximation from high-resolution lattice

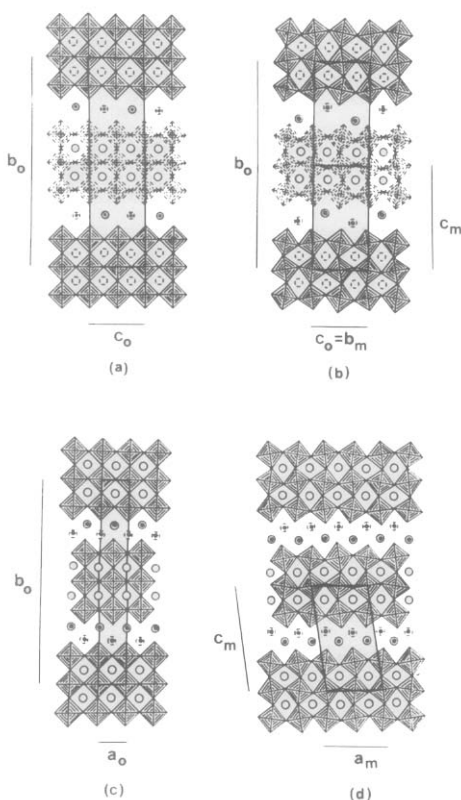


FIG. 3. Derivation of the structure model of monoclinic $\text{BaNd}_2\text{Ti}_3\text{O}_{10}$. (a) $[100]_o$ projection showing the ideal structure. The octahedra are not distorted or tilted and the symmetry is orthorhombic. (b) $[100]_o$ projection showing displaced Ba atoms due to the rotations of the octahedra about the x_o axis. (c) $[001]_o$ projection of the ideal orthorhombic structure with displaced Ba atoms. (d) Rotations of the octahedra about the z_o axis double the a_o axis repeat, and give a monoclinic structure. $[010]_m$ projection.

images and by taking only the strong reflections into account.

High-resolution electron microscopy of the $[001]_o$ projection showed bands of white dots (Fig. 4). The distance between the dots within one band is 3.8 \AA . The bands are shifted relative to neighboring bands due to the C -centering. From the high-resolution lattice images and the orthorhombic space group symmetry, an ideal orthorhombic structure could be derived.

The structure is based upon TiO_6 octahedra. The 3.8-\AA axis corresponds to the distance between the centers of two octahedra sharing corners. The ideal structure shown in Fig. 3a satisfies all three orthorhombic space groups $Cmc2_1$, $C2cm$, and $Cmcm$. The atomic parameters according to the highest symmetry space group $Cmcm$ are given in Table I.

In rutile, TiO_2 which has nearly regular TiO_6 octahedra the Ti-O distances vary between 1.95 and 1.98 \AA . If the octahedra in $\text{BaNd}_2\text{Ti}_3\text{O}_{10}$ are regular and all have the same orientation, the cell dimensions a_o and c_o would be in the ranges 3.90–3.96 and 7.80–7.92 \AA . The observed values are much smaller. Furthermore, the cation Nd^{3+} (ionic radius 0.995 \AA) is too small for the volume available with undistorted or untwisted octahedra. All this indicates that tilting of the octahedra probably occurs similar to perovskites. The tilting can be described as rotations about the three te-

TABLE I
ATOMIC PARAMETERS OF THE IDEAL
ORTHORHOMBIC $\text{BaNd}_2\text{Ti}_3\text{O}_{10}$ WITH
SPACE GROUPS $Cmcm$

Space group: $Cmcm$ (No. 63)			
$a_o = 3.8655 \pm 0.0003 \text{ \AA}$; $b_o = 28.156 \pm 0.003 \text{ \AA}$;			
$c_o = 7.6661 \pm 0.0007 \text{ \AA}$			
General positions: $16h (0\ 0\ 0, \frac{1}{2}\frac{1}{2}\ 0) +$			
	xyz	$x\bar{y}\bar{z}$	$xy\frac{1}{2} - z$
	$x\bar{y}z$	$\bar{x}yz$	$x\bar{y}\frac{1}{2} + z$
	x	y	z
4 Ba	4c	0.5	0.750
8 Nd	4c(1)	0.5	0.067
	4c(2)	0.5	0.933
12 Ti	4b	0.5	0.500
	8f	0.5	0.635
40 O	4a	0.5	0
	4c(1)	0.5	0.500
	4c(2)	0.5	0.365
	4c(3)	0.5	0.635
	8f(1)	0.5	0.567
	8f(2)	0.5	0.702
	8f(3)	0.5	0.135

trad axes with alternate octahedra twisting in opposite directions. If the octahedra can be assumed to be regular without distortions, the magnitude of some tilt angles can be deduced from the cell dimensions.

Figure 3b shows the effect of octahedral rotation about the x_0 -axis. The rotation angle is in the range 12–16°. Due to this rotation the Nd atoms have less than 12 nearest neighbors and the Ba atoms are displaced from ideal positions. The mirror symmetry normal to the z_0 axes can still be preserved. Figure 3c shows the $[001]_0$ projection of the ideal structure, but with displaced Ba atoms. Rotation of the octahedra about the z_0 axis gives a double repeat along the x_0 axis because alternate octahedra must twist in opposite directions. This effect explains the weak reflections in the electron diffraction patterns (Figs. 1b–d). The octahedral rotations and the new monoclinic unit cell are indicated in Fig. 3d. It is a characteristic feature of the monoclinic structure that the rotation of one octahedron determines the rotations of all the other octahedra. The rotation angle calculated from the cell dimensions is about 8–13°. It is to be noticed that such rotations about the z_0 axis can preserve mirror symmetry normal to the x_0 axis within each perovskite block, but the mirror symmetry of the orthorhombic unit cell is broken. The cell dimensions of the new monoclinic structure based on X-ray data are: $a_m = 7.7310 \pm 0.0006 \text{ \AA}$; $b_m = 7.6661 \pm 0.0007 \text{ \AA}$; $c_m = 14.210 \pm 0.002 \text{ \AA}$; $\beta_m = 97.82 \pm 0.01^\circ$.

Space Group Symmetry

A convergent beam electron diffraction (CBED) study by Olsen and Goodman (3) showed that some of the crystals contain mirror planes normal to both the a_0 and c_0 axes to a certain approximation. This indicates that the space group is *Cmcm*. A careful examination of the CBED patterns showed, however, that the symmetry

across the plane normal to the a_0 axis was broken in detail so that only the mirror symmetry across the plane normal to the c_0 axis was exact. All these observations were based only on the strong orthorhombic sublattice reflections because the weak reflections giving the monoclinic symmetry were lost beneath a high inelastic background and could not be examined directly with the normal CBED technique. However, the structural relationships which give the monoclinic symmetry have only a weak influence on the CBED discs of the strong reflections because their intensities depend mostly on the heavy atoms and are nearly unaffected by small displacements of the light atoms. On the other hand, because both the Ba and Nd atoms can be displaced along the y_0 axis without breaking the *Cmcm* symmetry (Table I), the intensity of the weak reflections has probably their main contribution only from the small displacements of the light atoms. In conclusion, it seems reasonable that the mirror symmetry normal to the z_0 axis is preserved by the octahedral rotation and the possible space groups of the monoclinic structure are No. 6 *Pm* or No. 11 *P2₁/m*.

These two space groups can be distinguished by the extinction rule for the 00 l reflections. For the *P2₁/m* space group the rule for the possible reflections is: 00 l : $l = 2n$, whereas for the space *Pm* there are no conditions. In the present case, however, this rule could not be tested directly due to the very weak reflections and dynamical electron scattering.

Olsen and Goodman (3) found by CBED that the intensity distribution in some of the reflections was consistent with the space group *Pm* and not *P2₁/m*. It is well known, however, that CBED patterns depend on the symmetry of the specimen and do not necessarily reflect the symmetry of the unit cell of the structure directly. If twin domains are present in the specimen the apparent symmetry as observed by CBED

TABLE II
ATOMIC PARAMETERS OF THE UNREFINED
MONOCLINIC STRUCTURE OF $\text{BaNd}_2\text{Ti}_3\text{O}_{10}$ WITH
SPACE GROUP $P2_1/m$

Space group: $P2_1/m$ (No. 11)					
$a_m = 7.7310 \pm 0.0006 \text{ \AA}$; $b_m = 7.6661 \pm 0.0007 \text{ \AA}$;					
$c_m = 14.210 \pm 0.002 \text{ \AA}$; $\beta_m = 97.82 \pm 0.01^\circ$					
Atomic positions:	$4f$	$x y z$	$\bar{x} \bar{y} \bar{z}$	$\bar{x} \frac{1}{2} + y \bar{z}$	$x \frac{1}{2} - y z$
	$2e$	$x \frac{1}{2} z$	$\bar{x} \frac{1}{2} \bar{z}$		
	$2b$	$\frac{1}{2} 0 0$	$\frac{1}{2} \frac{1}{2} 0$		
	$2a$	$0 0 0$	$0 \frac{1}{2} 0$		
		x	y	z	
4 Ba	$2e(1)$	0.131	0.250	0.524	
	$2e(2)$	0.631	0.250	0.524	
8 Nd	$2e(1)$	0.784	0.250	0.134	
	$2e(2)$	0.284	0.250	0.134	
	$2e(3)$	0.717	0.250	0.866	
	$2e(4)$	0.217	0.250	0.866	
12 Ti	$2a$	0.0	0.0	0.0	
	$2b$	0.500	0.0	0.0	
	$4f(1)$	0.068	0.0	0.270	
	$4f(2)$	0.568	0.0	0.270	
40 O	$2e(1)$	0.0	0.250	0.0	
	$2e(2)$	0.500	0.250	0.0	
	$2e(3)$	0.933	0.250	0.730	
	$2e(4)$	0.433	0.250	0.730	
	$2e(5)$	0.568	0.250	0.270	
	$2e(6)$	0.068	0.250	0.270	
	$4f(1)$	0.750	0.0	0.0	
	$4f(2)$	0.034	0.0	0.134	
	$4f(3)$	0.534	0.0	0.134	
	$4f(4)$	0.101	0.0	0.404	
	$4f(5)$	0.601	0.0	0.404	
	$4f(6)$	0.818	0.0	0.270	
	$4f(7)$	0.318	0.0	0.270	

Note. The Ba positions have been determined by matching lattice images.

may be lower than the actual symmetry of the unit cell within each twin domain. As already pointed out the monoclinic structure can be derived from the centrosymmetric orthorhombic $Cmcm$ structure by rotations of the octahedra. Furthermore, the rotation of one octahedron determines the rotations of all the other octahedra within the monoclinic unit cell. The origin of the monoclinic structure can be chosen at a Ti atom at a center of symmetry in the $Cmcm$ structure. Because all the tetrad axes which describe the rotation of the cor-

responding octahedron pass through this Ti atom, an inversion center is present also in the monoclinic structure. Therefore, the space group of the monoclinic unit cell is probably the centrosymmetric $P2_1/m$, whereas the symmetry of a specimen with twin domains can be noncentrosymmetric Pm depending on the distribution of twins.

Table II shows the atomic parameters of the $\text{BaNd}_2\text{Ti}_3\text{O}_{10}$ structure with the monoclinic space group $P2_1/m$. The values of the Ba positions have been determined by matching experimental and calculated high-resolution lattice images as shown in the next section, whereas the oxygen parameters are unrefined. The Nd and Ti atoms are in ideal positions.

High-Resolution Lattice Imaging

High-resolution lattice images were taken of three different projections. In the $[001]_0$ projection the octahedra in one perovskite-type block of the structure (Fig. 3c) are shifted relative to a neighboring octahedral block due to the C-centering. In the lattice image (Fig. 4) the blocks of bright dots are shifted relative to each other across the dark bands. According to the ideal structure model the Ba atoms are only 1.9 Å apart in this projection. Therefore, they are not expected to be resolved in the images, and they appear as dark bands. The Nd atoms appear as dark dots.

In the $[100]_0$ projection the lattice images (Fig. 5) give a reversal of the contrast compared to the $[001]_0$ projection. Now the Nd and Ba atoms appear as bright dots and the Ti octahedra as dark dots.

Lattice image of the $[1\bar{1}0]_0$ projection give no information about the detailed atomic arrangement in the unit cell, but demonstrate the $P2_1/m$ symmetry of the structure associated with the b_m axis (Fig. 6).

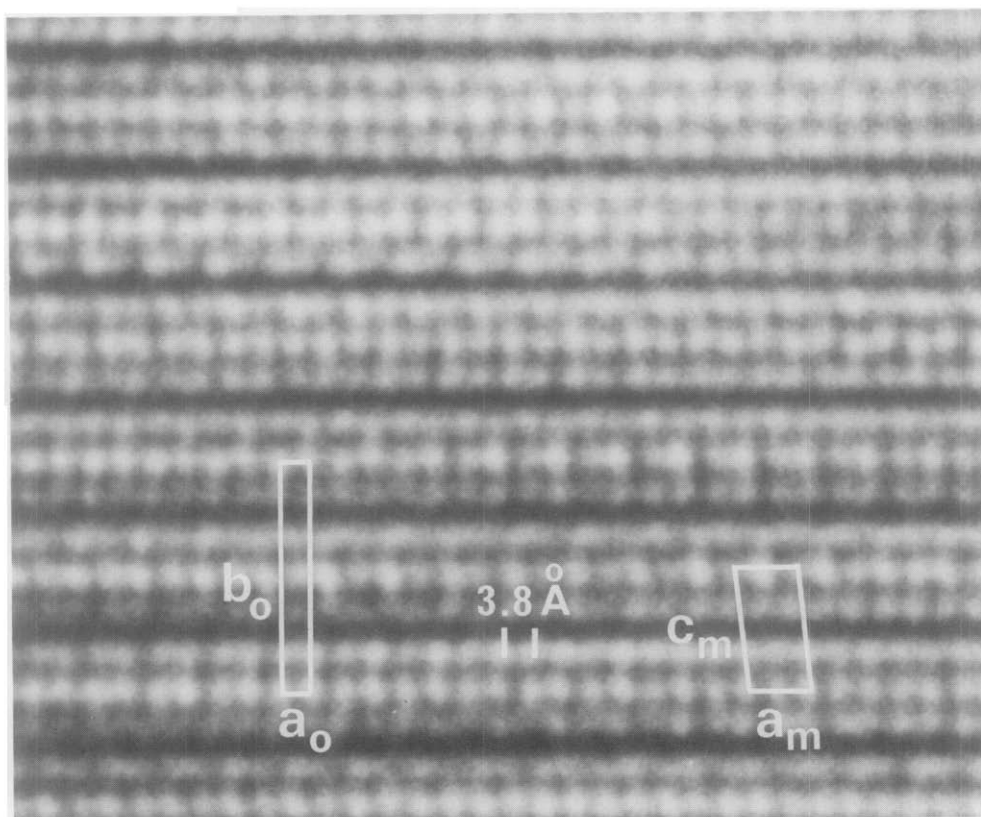


FIG. 4. Lattice image of the $[001]_0$ projection of $\text{BaNd}_2\text{Ti}_3\text{O}_{10}$. Each white dot corresponds to the Ti atoms in the TiO_6 octahedra. The orthorhombic and monoclinic unit cells are shown.

In order to confirm this qualitative interpretation high-resolution lattice images were calculated. The multislice formulation of the dynamical n -beam theory for the electron scattering was used (4, 5). Atomic scattering factors were obtained from Doyle and Turner (6). Through focus series were calculated for different crystal thicknesses t by taking into account spherical and chromatical aberration and beam divergence. The semiangle of the beam divergence was 1.4 mrad. The value 1.9 mm of the spherical aberration coefficient was determined by fitting calculated and experimental images of known structures. The effect of chromatic aberration was taken into

account by use of a damping envelope function. The computer programs were written by several workers at Arizona State University and the calculations were carried out at Oslo University using a Nord 10/50 computer.

Some calculated images of the $[001]_0$ and $[100]_0$ projections are shown in Figs. 7 and 8. Ideal positions were used for the oxygen, Nd, and Ti atoms. Calculations were carried out for several y_0 values of the Ba positions. The best fit between the experimental and calculated images was found for $y_0 = 0.762$ as demonstrated by comparing the Figs. 7c and 8b with Figs. 4 and 5. An exact agreement with the experimental images

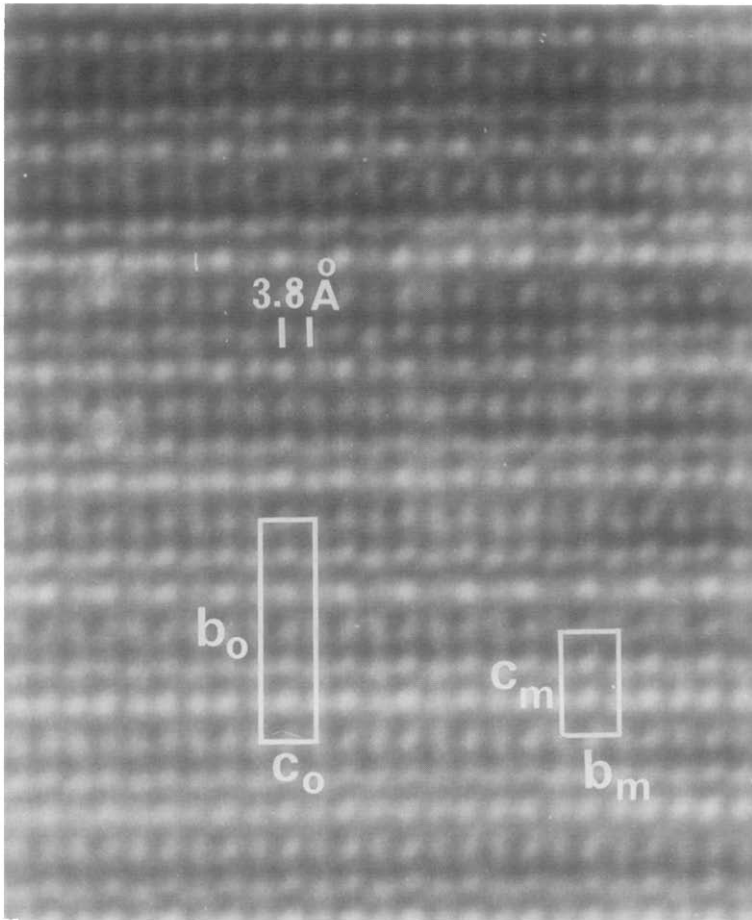


FIG. 5. Lattice image of the $[100]_o$ projection of $\text{BaNd}_2\text{Ti}_3\text{O}_{10}$ with the orthorhombic and monoclinic unit cells indicated.

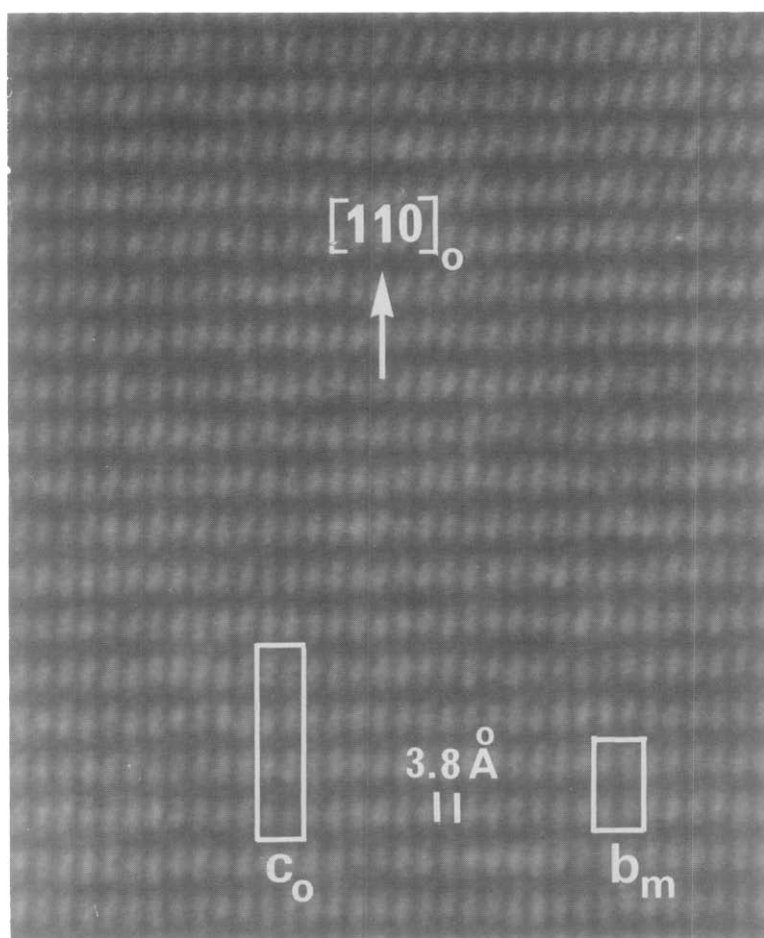


FIG. 6. Lattice image of the $[\bar{1}\bar{1}0]_o$ projection showing approximate $P2_1/m$ symmetry associated with the b_m axis.

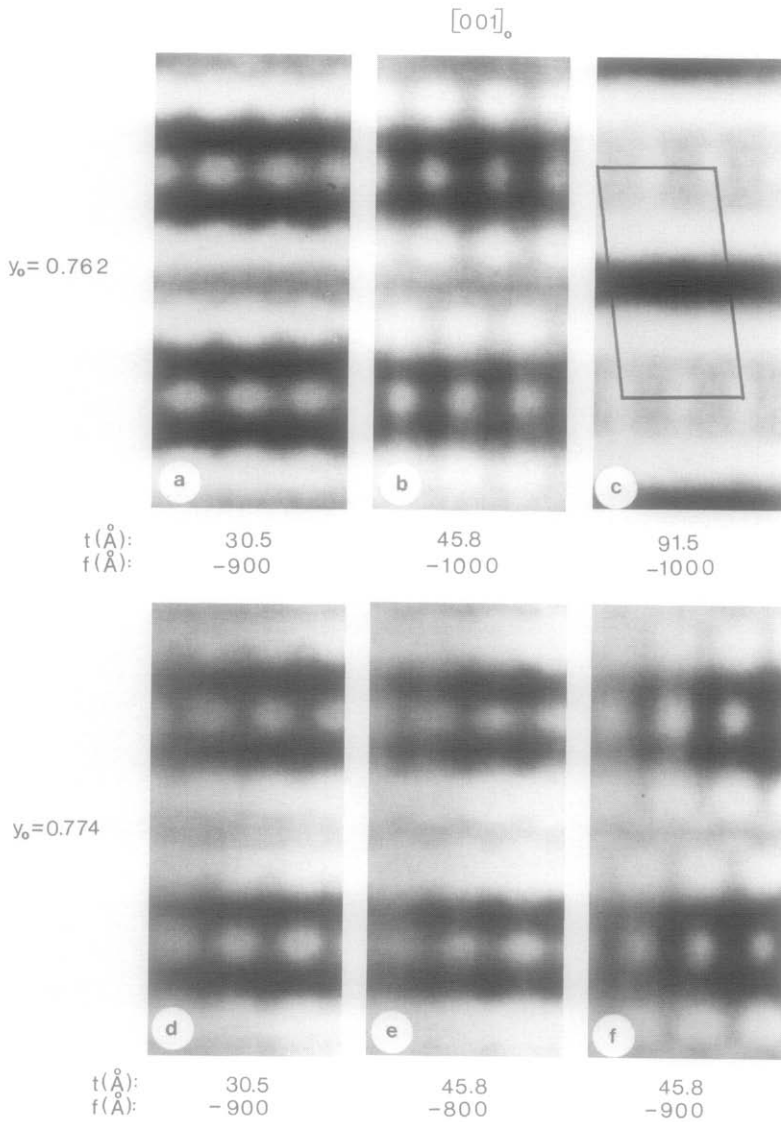


FIG. 7. Calculated lattice images of the $[001]_o$ projection of $\text{BaNd}_2\text{Ti}_3\text{O}_{10}$ for different defects of focus f and crystal thickness t . Figs (a-c) show calculations for $y_0 = 0.762$ for the Ba position. For the calculations shown in (d-f) the value for the Ba atoms was 0.774. The monoclinic unit cell is indicated in (c).

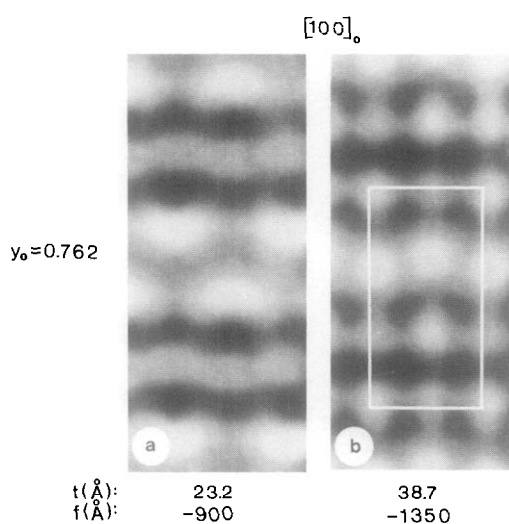


FIG. 8. Calculated $[100]_0$ lattice images of $\text{BaNd}_2\text{Ti}_3\text{O}_{10}$ for two different crystal thicknesses t and defects of focus f . The y_0 value for the Ba atoms is 0.762. The monoclinic unit cell is indicated in (b).

was not possible because only ideal positions were used for the oxygen, Nd, and Ti atoms.

Acknowledgment

The experimental work described in this paper was carried out at Arizona State University where one of us (A.O.) was supported on NSF Grant DMR8002108.

References

1. D. KOLAR, Z. STADLER, S. GABERSCEK, AND D. SUVOROV, *Ber. Deut. Keram. Ges.* **55**, 346 (1978).
2. D. KOLAR, S. GABERSCEK, B. VOLAVSEK, H. S. PARKER, AND R. S. ROTH, *J. Solid State Chem.* **38**, 158 (1981).
3. A. OLSEN AND P. GOODMAN, *Ultramicroscopy* **6**, 101 (1957).
4. J. M. COWLEY AND A. F. MOODIE, *Acta Crystallogr.* **10**, 609 (1957).
5. P. GOODMAN AND A. F. MOODIE, *Acta Crystallogr. A* **30**, 280 (1974).
6. P. A. DOYLE AND P. S. TURNER, *Acta Crystallogr. A* **24**, 390 (1968).